



LUND UNIVERSITY
Faculty of Science

Atmospheric soot particle transformation from urban to rural

Fredrik Johansson

June 28, 2018

Course: FYSK02

Project duration: 4 months

Supervised by:

Pontus Roldin

Joakim Pagels

Abstract

The main objective of this work was to investigate if there is a contribution of aerosol from the urban region of Copenhagen at the rural station Vavihill. This was done by analyzing measurement data between 1st of January and the 28th of February 2013 measured with a Differential Mobility Particle Sizer (DMPS), Soot Particle Aerosol Mass Spectrometer (SP-AMS), a Cloud Condensation Nuclei Counter (CCNC) and a NO_x-analyzer. To determine if the air masses passed over Copenhagen or not, the Hybrid Single-Particle Lagrangian Integrated Trajectory 4 (HYSPLIT4) was used to model air mass origin with six-hour intervals. The data consisted of measurements of particle number concentration, refractory black carbon (rBC) mass concentration, cloud condensation nuclei (CCN) concentration and NO_x concentration. The measurements showed a noticeable difference with higher concentration (rBC: 33 %, CCN: 30-42 %, NO_x: 58 %) and a larger number concentration of particles (36%) for the air masses passing over Copenhagen. The analyzed time series were too short to find statically significant contributions from Copenhagen to the aerosol composition in Vavihill. To determine if there really is a significant contribution of aerosol from the urban region of Copenhagen at the rural background station Vavihill, further investigations should be made.

Contents

1	Introduction	2
2	Aerosols and particles	3
2.1	Particle sources	3
2.2	Chemical structure	4
2.3	Hygroscopic properties	5
2.3.1	Cloud formation	6
2.3.2	Köhler theory	6
2.4	Deposition	8
2.5	Aging of soot particles	9
2.6	Impact on the climate	9
2.6.1	Direct effect	9
2.6.2	Indirect effect	10
3	Method	10
3.1	SP-AMS	10
3.2	CCNC	11
3.3	DMPS	11
3.4	NOx-analyzer	12
3.5	HYSPLIT	12
4	Result and discussion	14

1 Introduction

In all the environment there are particles swirling around in the air. These particles are called aerosol particles, which means particles suspended in gas. The size of the particles spans several orders of magnitude in diameter, from ~ 1 nm up to ~ 100 μm [1].

Aerosol is found in all of the atmosphere with highest concentrations in the lowest part which is called the troposphere. The troposphere extends to 7 to 20 km above sea level, depending on the location on earth [2]. The particles can be in either a solid or liquid phase and are characterized by their ability to maintain suspended in the gas for a long time [3].

Eruptions from volcanoes, pollen dispersal and combustion of fossil fuel are only a few of the physical, chemical and biological processes that produce aerosols. One important source of aerosols in urban regions is traffic. The exhausts from vehicles are constantly producing millions and millions of particles and molecules that find their way in to the air in our environment [4]. This airborne pollution consists of a variety of gas molecules (ozone, nitrous oxide, sulfur dioxide, carbon monoxide) and particles, including soot [5].

Soot, or black carbon, is produced from incomplete combustion. It is emitted from various sources including diesel cars and trucks, forest fires and agricultural open burning [3]. Black carbon particles play a substantial part in climate change by absorbing solar radiation and re-radiating the energy as heat, warming the local atmosphere [6]. But most aerosol do not have a warming effect on the climate. There are multiple different aerosols that influence the cloud albedo. Albedo is a measure of reflectivity or the proportion of radiation reflected from an illuminated surface. The properties of the droplets in the cloud is the most important factor for the cloud albedo and is affected by a large number of variables. The sizes, the composition and the number of droplets are the most prominent of these variables [7].

In this study, the main goal is to examine if there is a noticeable difference in the proportion of soot and number of cloud-forming particles from the urban region of Copenhagen compared to air not influenced by Copenhagen. This was done by studying air masses at the rural station Vavihill in the northwest part of Scania. The data for this study are taken from the rural station Vavihill and were analyzed for the period from 1st of January to the 28th of February 2013. The data consists of measurements from a Soot Particle Aerosol Mass Spectrometer (SP-AMS), a Cloud Condensation Nuclei Counter (CCNC), Differential Mobility Particle Sizer (DMPS) and a NO_x-analyzer.

The research questions that have been investigated in this study are:

- Is there a significant difference in the particle number size distributions between the air masses influenced and not influenced by Copenhagen?
- Is it possible to detect a difference in the concentrations of soot between the air masses influenced and not influenced by Copenhagen?
- Is the amount of cloud condensation nuclei different in the air masses influenced and not influenced by Copenhagen?

2 Aerosols and particles

As mentioned in the introduction, aerosol particles span many orders of magnitudes in size, from around 1 nm up to 100 μm . The lower limit is determined by that aerosol particles must consist of molecular clusters of more than a few single molecules and the upper limit is determined by the sedimentation rate, which is further described in section 2.4 [3].

From this definition it is possible to conclude that all of the Earth's atmosphere can be considered an aerosol.

2.1 Particle sources

Depending on the source, the particles are divided into two different categories: primary and secondary aerosol particles [8].

Primary aerosol particles are particles that are created directly from a source. A good example of this is soot particles which are produced from incomplete combustion. Secondary aerosol particles on the other hand are created through gas-to-particle conversion. They are formed a time after the gases have been released into the air from both human pollution and natural sources. The main processes for the formation of these secondary aerosol particles is nucleation, condensation and coagulation, **figure 1** [3].

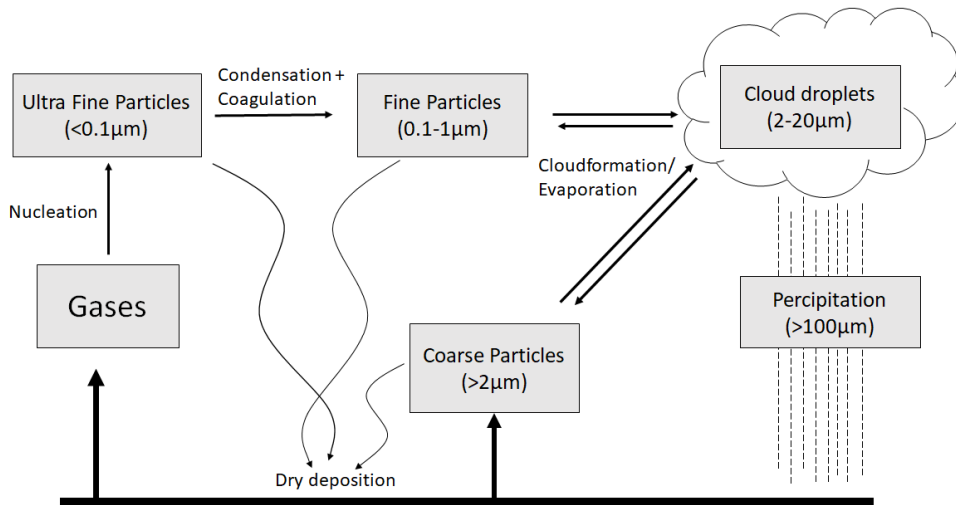


Figure 1: Schematic overview of the flow of aerosol between different states and in different phases. Nucleation form particles that are around $0.001-0.002\mu\text{m}$ and then they start to grow by condensation or coagulation to ultra-fine particles.

Condensation is the most common and most important process of particle growth in the atmosphere. The process transfers mass from the gas phase to the particulate phase and requires vapor that is supersaturated relative to the particle. Supersaturation is when a vapor of a compound has a higher partial pressure than the vapor pressure of that compound. For water vapor, air is referred as saturated when the partial pressure for water equals vapor pressure over a clean flat water surface in equilibrium with the air. The reference state is thus the partial pressure of water over a clean water surface. In this case the air is supersaturated by a certain substance with regard to what had been the case if there

was a balance between the gas phase (air) and the aerosol particles. One way of achieving this is for the solute to be cooled from a higher temperature to a temperature below that at which saturation occurs [1]. The process of particle growth by condensation is initiated by particles that allows water vapor, or other gases, to condensate onto their surfaces.

Coagulation of aerosols is the process of particles colliding and adhere to each other to create larger particles. As the particles stick to each other the number of particles decreases and the size of the particles increases [1]. There are two different types of coagulation: thermal coagulation and kinetic coagulation. Thermal coagulation is due to the relative motion between the particles being a Brownian motion. The thermal coagulation is spontaneous and constantly occurring in the aerosols. Kinetic coagulation is a result of relative motion due to external forces, such as gravity or electrical forces [3]. The process of coagulation is the most important phenomenon for interparticle interaction in aerosols [1].

Nucleation is divided into two types: heterogeneous and homogeneous. Heterogeneous nucleation is the formation process of particles in the presence of condensation nuclei or ions. The process is the primary process in the formation of clouds, further described in section 2.3.1 [1]. Homogeneous nucleation is the formation of particles from supersaturated vapor without the assistance of condensation nuclei or ions that are required in heterogeneous nucleation. The process is initialized by the vapor, or gas, forming clusters of molecules. The clusters are unstable and continuously disintegrated and new clusters are formed. As the saturation of the vapor increase the concentration of clusters increase and as the concentration increases the clusters start to collide with one another and create agglomerates. If these agglomerates reach a certain activation diameter, depending on the vapor or gas, it becomes stable and then starts to grow by condensation [9]. This process is similar to coagulation with the exception of that the agglomerates disintegrate rapidly after their formation and that it is gas molecules, not particles, that collide [1].

It is very hard to estimate the contribution of aerosols from many of the natural sources. This problem comes from that it is difficult to identify and track aerosol particle from these sources. The situation is similar with the anthropogenic sources, such as pollution from industrial areas. These have been studied far more extensive and even though some have been well established most are still very uncertain [6].

This uncertainty makes it more difficult to estimate and model the distribution of aerosol and the effects they have on the climate [3].

The size of the particles is very decisive for the characteristics of the aerosol, especially transport and deposition. Particles that origin from mechanical processes, such as sea spray and erosion, tend to have a larger diameter, up to $\sim 10 \mu\text{m}$, whereas most combustion particles are smaller than 100 nm. Secondary particles created by nucleation has an initial diameter of 1-2 nm [10].

2.2 Chemical structure

Particles that originates from combustion of fossil fuels or natural sources such as forest fires most commonly contain organic carbon and elemental carbon. The elemental carbon particles (soot) form aggregates which means that they fuse into chains with organic, and

sometimes with metal, matter along the surface. The chains have a length of about 50-200 nm [6].

Another type of particles that are dominant in exhausts are particles that are formed from condensation of incompletely combusted hydrocarbons within seconds after emission when the gases cool down in the air. These particles are mostly made up of primary organic aerosol and sulfates [6, 11].

The secondary particles that are formed from condensation are characterized by the gases that they originated from. Sulfur dioxide is one important gas that has been established to be strongly linked to nucleation. It originates from a variety of combustions and volcanoes and oxidizes to sulfuric acid which easily condenses into liquid sulphate particles due to low vapor pressure. In addition to sulfuric acid, nucleation is also believed to be done by means of organic substances [8]. The composition can then be changed when other gases condense on the new particles. As the aerosol particles that have been released into the atmosphere go through different transformation processes, the compounds of the particle soon consist of many different chemical substances. Although these processes add a variety of substances they tend to make particles of similar size become more and more like each other. When the particles in a gas are composed of identical substances, the mixture is said to be an internal mixture [2].

This continuous process of mixing makes it very difficult to see the difference between and determine the content of both primary and secondary particles. Thus, it is difficult to track the origin of a particle after it has aged for some time in the atmosphere, described in section 2.5.

Another type of mixing is external mixing. In contrast to internal mixing, where every particle in the mixture has identical composition, an external mixture is composed of particles with different composition [2].

2.3 Hygroscopic properties

When studying aerosols and their impact on the climate and human health, the hygroscopic properties are very important. Hygroscopicity is the ability to absorb and emit water. Since the particles in the atmosphere are constantly surrounded by and interacting with water molecules, the way water affects the properties of the particles is an essential aspect to look into more closely [4].

As mentioned before aerosol particles can be both solid and liquid. A substantial part of the liquid particles contains compounds that dissolve in water e.g. sulphates, nitrates and chlorides. These compounds enable water to be absorbed at relatively low humidity. The aerosol particles are said to be hygroscopic. At a certain relative humidity, depending on the compound, the particles start to take up water and form concentrated liquid drops. This humidity is called the deliquescence point. When the humidity decreases the drop size decreases due to evaporation and finally the drop crystallizes. This is a common feature of inorganic salts such as sulfates, nitrates and chlorides [3, 4].

2.3.1 Cloud formation

Atmospheric aerosols have important effects on the formation of clouds as well as their properties. Except for the humidity, the size distribution and composition of the particles are two of the most prominent factors.

The growth of particles in the atmosphere is mainly depending on the humidity in the surrounding air, as mentioned in the previous section. Cloud droplets are formed out of Cloud Condensation Nuclei (CCN) that become activated and the particles start to take up water, mostly through condensation, and finally becomes liquid drops.

To activate the CCN to cloud droplets the relative humidity in the air has to increase and become supersaturated. One example of this is when air rises to pass over a mountain and creates clouds. As the relative humidity rises the activated CCN grow in sizes to $\sim 20\mu\text{m}$, compared to the particles that is not activated as CCN grow only 1-10 times their initial diameter of $<0.1\mu\text{m}$, ultra-fine particles, see figure 1 [12].

As mentioned, both size distribution and composition of the aerosol particles have an impact on the formation [13]. The size distribution is the substantial factor and explains almost 80% of the variation in activated CCN [7].

The composition is the second most prominent factor in the activation of CCN. The fact that cloud droplets make up a large surface area, make them absorb water soluble gases in a very efficient way. Some of these soluble gases gain a higher rate of oxidation in aqueous solutions than they have in their gas phase. This causes a large part of the compound to oxidize even though the cloud droplets have a relatively short lifetime [7].

A majority of the droplets in the clouds evaporate before they reach a size which will lead to precipitation. It is estimated that particles go through the process of forming clouds and evaporating an average of 10 times before they are removed by precipitation and for each time the particles form drops the surrounding gases are absorbed into the drops. This changes the composition and the particles become larger and more internally mixed [12].

2.3.2 Köhler theory

The activation of CCN into cloud droplets can be described by Köhler theory. Köhler effect combines Raoult's law with the Kelvin effect and is one of the most important equations in the field of cloud microphysics [3].

Raoult's law comes from thermodynamics and relates the saturation vapor pressure to the solute. For a single component in an ideal solution Raoult's law states

$$p_i = p_i^* x_i \quad (1)$$

where p_i is the partial vapor pressure of the component i in the gaseous mixture, p_i^* is the pure-liquid saturation vapor pressure of the component i , and x_i is the mole fraction of the component i in the mixture [14].

Since the surface of the droplets are curved, the droplets can be regarded as a sphere. This approximation makes it possible to apply the Kelvin effect. The Kelvin effect describes the change in vapor pressure due to a curved surface.

$$\ln\left(\frac{p}{p_m}\right) = \frac{4M_w\sigma_w}{RT\rho_w D_p} \quad (2)$$

where p is the saturated vapor pressure for the substance over a curved surface, p_m is the saturated vapor pressure for the substance over a flat surface, σ_w is the surface tension, M_w is the molecular weight of the pure liquid, ρ_w is the density of the liquid, R is the universal gas constant, D_p is the diameter of the droplet, and T is the temperature [1].

When combining Raoult's law, eq.1, and the Kelvin effect, eq.2, the Köhler equation can be derived:

$$\ln\left(\frac{p_w(D_p)}{p_i^*}\right) = \frac{4M_w\sigma_w}{RT\rho_w D_p} - \frac{6n_s M_w}{\pi\rho_w D_p^3} \quad (3)$$

Where p_w is the saturation water vapor pressure, p_i^* is the corresponding saturation vapor pressure over a flat surface of pure water, σ_w is the droplet surface tension, ρ_w is the density of the pure water, n_s is the moles of solute, M_w is the molecular weight of pure water, and D_p is the cloud drop diameter [3, 14].

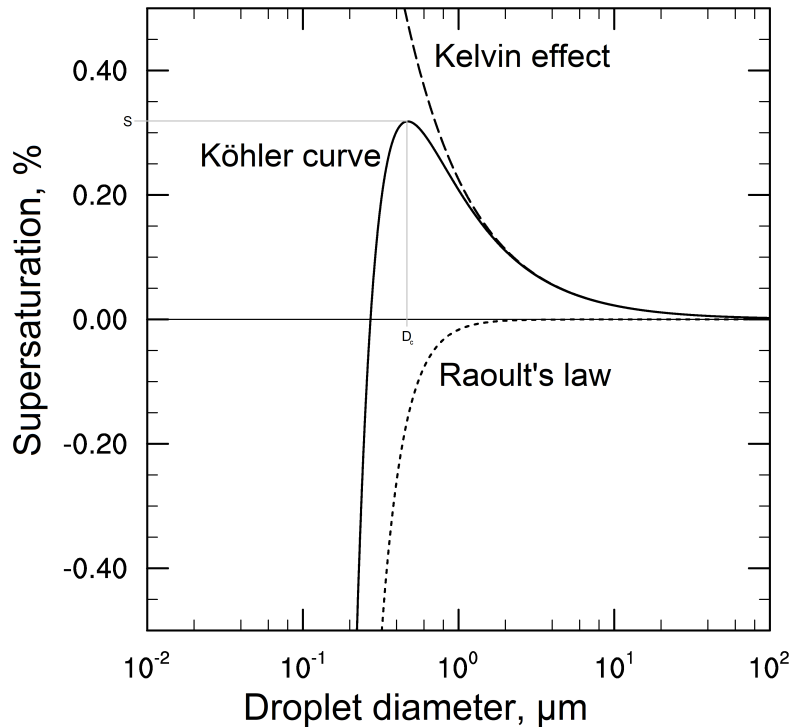


Figure 2: The Köhler curve, which is a visual representation of the Köhler equation (Eq.3). The curve describes the droplet diameter as a function of supersaturation. S denotes the critical supersaturation, D_c denotes the critical diameter. [15]

The Köhler curve, figure 2, is the curve that visually represents the Köhler equation, eq.3. It describes the supersaturation that is needed for the particle to grow into a cloud droplet.

For diameters smaller than the critical diameter, D_c , the Raoult's law ($-1/D_p^3$) is stronger than the Kelvin effect. As the diameter gets larger, the Kelvin effect ($1/D_p$) takes over and becomes the dominant term. The particle continues to grow with the supersaturation until it reaches the critical supersaturation, S . The particle cannot activate and become a cloud droplet until the supersaturation exceeds S . If the supersaturation reaches S the droplet can grow larger than the critical diameter D_c , which is the diameter of activation for the droplets. Drops that reach this diameter can activate and grow into a cloud drop even if the saturation is constant or reduces and those particles that do not reach this diameter will not activate [3, 16, 1] .

The critical supersaturation and the critical diameter is dependent of the amount and composition of the solute. This makes the exact shape of the curve different depending on the solute in the drop. Drops with a larger amount of solute have a lower critical supersaturation and are thus more likely to activate into cloud drops [3, 7].

2.4 Deposition

Particles are deposited on the ground or other surfaces. Deposition can happen either through dry deposition or wet deposition. Collisions and merging of particles are not included in deposition [3].

The main processes that are important for dry deposition are: sedimentation, impaction and diffusion.

Large particles, particles that are larger than $20\ \mu\text{m}$, are mainly deposited by sedimentation. Suspended particles have a tendency to settle due to different forces such as electromagnetism, centrifugal acceleration or, the most common, gravity. Sedimentation is when the settling process end and the particle rest against a surface.

In an aerosol that do not stream in a straight line, particles have difficulties to follow the path of the gas. This may cause the particles to collide with objects that the gas streams around. This is called impaction. One example of this is when the wind blows through the branches of a tree. Impaction is the dominating type of deposition for particles in sizes between ~ 1 to $\sim 20\ \mu\text{m}$ and deviation from the aerosols trajectory becomes larger the larger the particle are [3].

For particles smaller than $0.1\ \mu\text{m}$, diffusion is the most important form of deposition. Diffusion occurs when particles have a Brownian motion relative to the surrounding gas and therefore are brought to the surface [1].

Wet deposition is when the particles are either incorporated in cloud drops or precipitation. As clouds begin to precipitate, the particles are brought down to the ground. This processes in clouds that results in wet deposition are called *rainout* [3]. The other type of wet deposition is when falling rain drops collide with the suspended particles and remove them from the air [3, 12]. Wet deposition is highly dependent on meteorological conditions such as air temperature and humidity, wind velocity and mixing [12].

2.5 Aging of soot particles

As soot particles, described in section 2.2, are transported in the atmosphere through a multitude of processes, they are transformed. This transformation is sometimes referred to as aging [17]. Aging has several important effects on the particles properties.

When the soot particles are freshly emitted into the air they are hydrophobic, i.e. non-hygroscopic, and highly aspherical [18]. The fresh particles are present in an external mixture, described in section 2.2, which over time can change due to coagulation and condensation. As the aerosol get more and more internally mixed the hygroscopic portion of the aerosol particles increases and the fraction of black carbon content decreases [19].

The effect of this change in composition of the particles, is that the optical properties of the aerosol is altered. The absorption and scattering of light is amplified due to the condensation of other compounds onto the soot particles [20]. This results in the intensity of a beam of light that passes through an aerosol diminish to a larger extent and the visibility is reduced. Visibility is a measure of the distance where light or an object can be seen clearly. The reduction in visibility is one of the most apparent evidences of air pollution [3, 1]. The supersaturation required for the soot particles to activate into cloud droplets and form clouds is also affected. Since the fresh soot is hydrophobic it is unlikely that the particles will contribute to the number of CCN. Due to the process of aging the structure of the soot particles become more compact and the hygroscopic properties are enhanced [10].

2.6 Impact on the climate

Both natural and anthropogenic, primary and secondary aerosol particles have an effect on the climate. However, it is not trivial to show trends and longtime effects of aerosol since there are large variations in the atmospheric aerosol and, as mentioned in section 2.1, the emissions from various sources are uncertain [6]. The difficulty is further increased by aerosols not only having a warming effect but primarily a cooling effect [21].

2.6.1 Direct effect

The direct effect is cause by the scattering and absorption of solar radiation by the aerosol. How effective the scattering of radiation depends on the size of the particles. The scattering is most effective if the aerosol consists of particles that have the same radius as the wavelength [22]. This results in a larger portion of the solar radiation to be scattered back into space. From this follows that with a higher amount of particles in this range, the earths albedo increases, which has an cooling effect on the climate [23, 6]. The thermal radiation from the earth consists of radiation of a higher wavelength and is thus not scattered in the same extent by the aerosol [22].

Despite that the thermal radiation is not scattered it is still highly relevant for the climate. Some particles, e.g. soot, absorb the solar and the thermal radiation from the earth and warm the surrounding air. This absorption has a warming effect on the climate and is called the semi-direct effect [6]. As the particle heat up the surrounding air it affects the condensation of the water vapor, resulting in a decrease in formation of clouds [24].

When soot particles are activated as CCN, they eventually part fall to earth as rain or snow. This darkens the surface and reduce the surfaces ability to reflect the radiation from the sun and especially has severe impacts on the parts covered by snow and ice. This process increases the warming of the snow and further intensifies the melting rate. As this process continues, the grains of snow stick together as the snow melts and refreeze. As the snow grains gets bigger, more radiation is absorbed, and thus the melting rate increase [10, 6, 24].

2.6.2 Indirect effect

The clouds ability to reflect sun light, its albedo, is affected by the number of particles. Hence, the larger concentration of aerosol that act as CCN the higher is the clouds albedo. This is called the Twomey effect and has a cooling effect on the climate [21].

But it is not only the albedo that is affected by aerosols, but also the lifetime of the clouds. When there is a higher concentration of particles the water is distributed over a larger amount of particles. This results in smaller droplets the higher the particle concentration is. Since the particles is smaller in size there are less collisions inside the cloud that will result in droplets large enough to form precipitation. The time before the clouds are emptied on precipitation and dissolved thus becomes longer, which results in a cooling effect [21].

To conclude if the net-effect the aerosols have on the climate is cooling or warming, all these processes and effects must to be taken into account, both direct and indirect. This is still very uncertain and is currently a very active field of research [6, 24].

3 Method

The measurements taken at the rural station at Vavihill was performed with SP-AMS, CCNC, DMPS and NOx analyzer. The determination of where the air masses come from was done with the program HYPPLIT4 which was used to simulate the backwards trajectories of the air masses.

3.1 SP-AMS

The SP-AMP is a Aerosol Mass Spectrometry (AMS) with an additional module called Single Particle Soot Photometer (SP). A regular AMS vaporizes the aerosol particles thermally at ~ 600 °C with a resistively heated vaporizer, more commonly referred to as a tungsten vaporizer. When the particles have been vaporized they are ionized with the help of an electron beam. The ions that are generated are then detected in a high-resolution mass spectrometer. Although the AMS is a very useful method it does not include detection of refractory aerosol components, which includes soot particles [25].

Refractory components contains material that absorb light very effectively. To be able to detect these refractory components in the aerosol, the SP-AMS was developed. The SP-AMS is as mentioned an AMS with a additional SP module. Instead of the tungsten vaporizer, used in a standard AMS, the SP-AMS uses a laser vaporizer to vaporize the particles containing material that is refractory before it reaches the tungsten vaporizer. This allows the device to characterize the refractory components of the aerosol. The laser vaporizer and the tungsten vaporizer does not interfere with each other which makes it possible to use them both at the same time or independently of each other [25].

3.2 CCNC

A Cloud condensation nuclei counter, CCNC, measures the concentration of CCN particles and is a cylindrical continuous-flow thermal-gradient diffusion chamber. The CCNC lets the aerosol flow into a column which contains supersaturated water vapor. This condition of supersaturation is created by using the difference in diffusion rates between the heat and the water vapor. This difference makes the water vapor diffuse, at a higher rate than the heat, from the warm and wet wall of the column and move towards the center of the cylinder. Since the temperature gradient on the wall is controlled, this creates a supersaturation that can be modified along the centerline. Measurements from the CCNC are represented as a supersaturation spectrum, which is the number of CCN as a function of the supersaturation of the water vapor [26].

3.3 DMPS

A Differential Mobility Particle Sizer, DMPS, consists of two parts: a Differential Mobility Analyzer (DMA), figure 3, and a Condensation Particle Counter (CPC).

Before the particles reach the DMA, they go through a neutralizer. In the neutralizer the particles are exposed to high concentrations of positively and negatively charged ions that collide with the particles. This leads to a well-defined equilibrium charge distribution. The DMA then separates the charged particles according to their electrical mobility in an electric field. The electrical mobility is the particles ability to move through a medium that is exposed to an electric field. The particles specific electrical mobility, eq. 4, is dependent on the particles charge and diameter.

$$Z = \frac{qC_c}{3\pi\eta D_p} \quad (4)$$

Where Z is the electrical mobility, q is the charge of the particle, D_p is the mobility diameter of the particle, η is the dynamic viscosity of the air and C_c is the Cunningham slip correction factor, which is used when calculating the drag on small particles when having to account for noncontinuum effects.

The separation is done by letting the aerosol flow through a cylindrical capacitor with a inner electrode, in the shape of a rod in the center of the cylinder, and an outer electrode along the walls of the cylinder. The electrodes create an electrical field in the space in between them. As the aerosol flows the particles move towards the rod at a velocity that is dependent on their electrical mobility. Particles with a certain velocity will exit through

a slit in the end of the cylinder and the rest, with higher or lower velocity, will either deposit on the rod or exit with the exhaust flow [27, 28].

The particles that exit the DMA through the slit then enters a CPC which counts the particles. The counting process starts by making vapor condense on the particles making them grow into large droplets. This makes the particle large enough for detection by a laser beam. The instrument is able to detect particles between $\sim 3\text{-}800\text{ nm}$ [27].

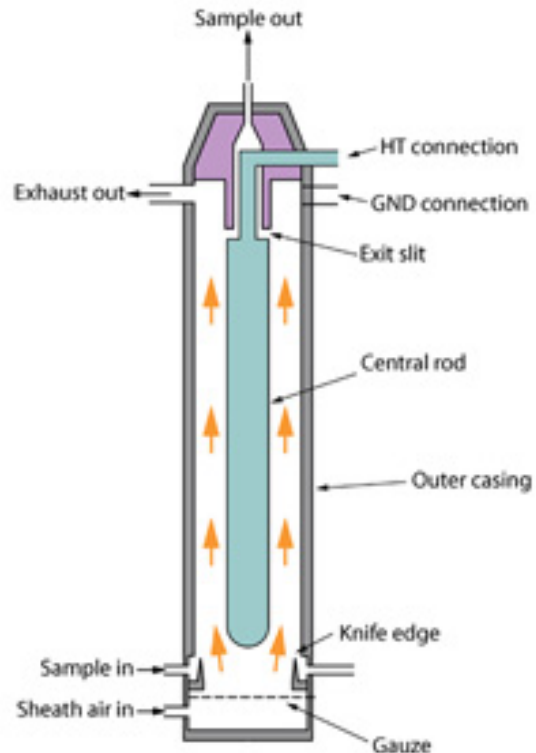


Figure 3: Schematic diagram of a differential mobility analyzer, DMA [29].

3.4 NO_x-analyzer

The NO_x-analyzer is a device for measuring NO and NO₂. The instrument uses two chambers, measuring NO directly and then NO₂ indirectly. In the first chamber the detection of NO is done. The air then goes to the second chamber which is a heating catalyst chamber that converts the NO₂ into NO. Measurements of NO are then taken again and the difference in the two measurements makes it possible to determine the amount of each component [30].

3.5 HYSPLIT

The Hybrid Single-Particle Lagrangian Integrated Trajectory (HYSPLIT) model is a system for modeling trajectories of air masses. To determine if the sampled air masses had passed Copenhagen on its way to the rural station Vavihill, the latest version HYSPLIT4 was used [31].

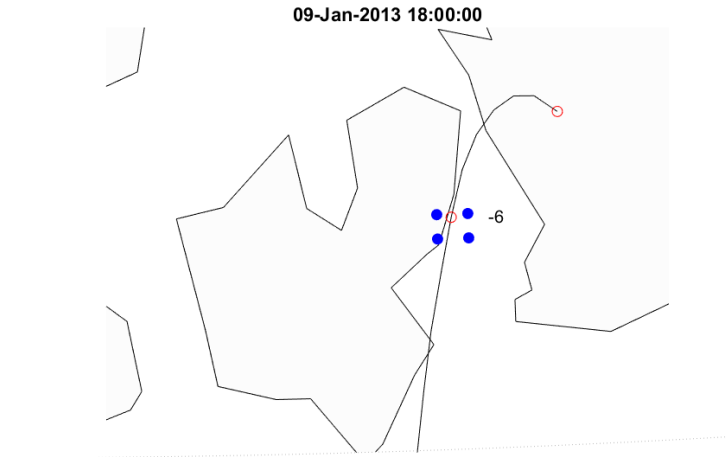


Figure 4: Map generated from the data from HYSPLIT trajectory modeling of January 9, 2013, 18.00. The four blue dots are the corners of the square over Copenhagen made at the latitudes and longitudes: (55.717, 12.468), (55.643, 12.468), (55.643, 12.637) and (55.717, 12.637). The red circle is the longitudes and latitudes of the air masses every six hours. The fitted black line to the hourly longitudes and latitudes is the trajectory of the air masses which ends at the rural station Vavihill. Since the map is generated by the program and not an exact map, the coastal line does not match the real longitudes and latitudes of the landmass. This results in the blue square to visually seem to be partly in the ocean.

The calculation of forward and backward trajectories, made by HYSPLIT4, allows for the representation of airflow patterns to interpret the transport of pollutants over different spatial and temporal ranges. By grouping trajectories that have similarities in path traveled it is possible to simplify the analysis, interpretation and determination of transport pathway in the atmosphere [31].

A square, made up of four point of latitudes and longitudes for the area over Copenhagen, was marked in the map, as seen in figure 4. The area covered by the square was chosen to cover the three large roads O2, O3 and E20 and Copenhagen airport, which all are large sources of emission in the region. If the trajectory passed through this square before reaching the rural station at Vavihill it was marked as "with CPH" otherwise it was marked "without CPH".

Since the HYSPLIT model had an interval of one hours for each new point of the trajectories the identification was made visually by identifying when the trajectories passed through the square representing Copenhagen.

The trajectories modeled arrived at Vavihill at the height of 100 m above ground and was modeled for 72 hours backwards in time. The meteorological data used for the calculation of the trajectories were provided by the National Weather Service's National Centers for Environmental Prediction (NCEP) Global Data Assimilation System (GDAS).

4 Result and discussion

To determine if there was a difference in the particle number size distributions in the air masses that passed and did not pass Copenhagen, both the mean and median of "with CPH" and "without CPH" was compared. As can be seen in figure 5, the median number concentration of particle for "with CPH" was consistently higher for particles with diameters of 12-550 nm with differences up to about 105 %. This higher number concentration was further supported by the mean of the total number of particles, seen in table 1, which was 36 % higher for "with CPH" compared to "without CPH". This indicates that the air passing over Copenhagen is influenced by urban emissions.

The result does however not exclude the possibility that the particles originated from other urban regions. This is due to that the identification of the HYSPLIT trajectories did not take into account the path the air masses travel before they reached Copenhagen. Therefore, urban regions in the northern part of Europe might have a significant impact on the result. This is further supported by the analysis of the trajectories. The trajectories were modeled for every six hours from January 1st to February 28th 2013. This corresponds to a total of 236 trajectories. Out of these 236 trajectories there was only 16 that passed over Copenhagen, where 13 out of the 16 coincided with trajectories that passed over the northern part of Europe or Malmö. The remaining three trajectories coincided with open water.

Table 1: Means and standard deviations of the total number of particle, rBC mass concentration and NO_x concentration for air masses that passed ("with CPH") and not passed Copenhagen ("without CPH") measured at the rural station at Vavihill. The means are for the 6-hour interval labeled after HYSPLIT trajectory analysis.

	"With CPH"	"Without CPH"
Mean total number concentration of particles, N	4366 ± 2232	3217 ± 2795
Mean rBC mass concentration, ng/m^3	16.61 ± 13.31	12.45 ± 16.22
Mean NO _x concentration, ppb	5.83 ± 3.24	3.69 ± 2.53

Furthermore, the deviations in the result is very large. As can be seen in figure 5, there is a large overlap in the 25-percentile bands of "With CPH" and "Without CPH". This overlap illustrates the large variability and makes the result have no statistical significance.

The influence of urban emission on the air passing over Copenhagen is further manifested in the amount of rBC, NO_x (table 1) and CCN (table 2). Comparing the mean rBC mass concentration showed that air masses passing over Copenhagen had a 33 % higher amount for the 6-hour intervals (table 1) than the air masses not passing over Copenhagen. The standard deviation of the mean rBC mass concentration do, however, show that the spread of the measured data is large. The mean NO_x concentration (table 1) was 58 % higher for the air masses passing over Copenhagen. The NO_x data showed the same characteristics as the number of particle and rBC mass concentration with a large difference with large deviations. The differences in the measured particle and NO_x concentration with and without Copenhagen is not statistically significant.

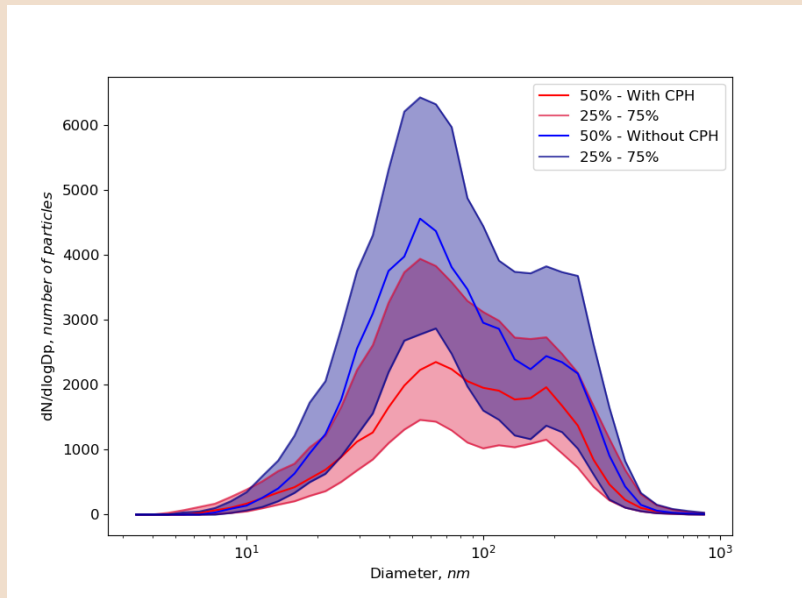


Figure 5: Comparison of the median number of particles, $dN/d\log(D_p)$, as a function of the particle diameter, nm, between the air masses "with CPH" (Blue) and "without CPH" (Red) with quartile bands. $dN/d\log(D_p)$ is the normalized concentration. dN is the number of particles in the range (total concentration) and $d\log(D_p)$ is the difference in the log of the channel width. $d\log(D_p)$ is calculated by subtracting the log of the lower bin boundary from the log of the upper boundary for each channel and thus normalizing for bin width.

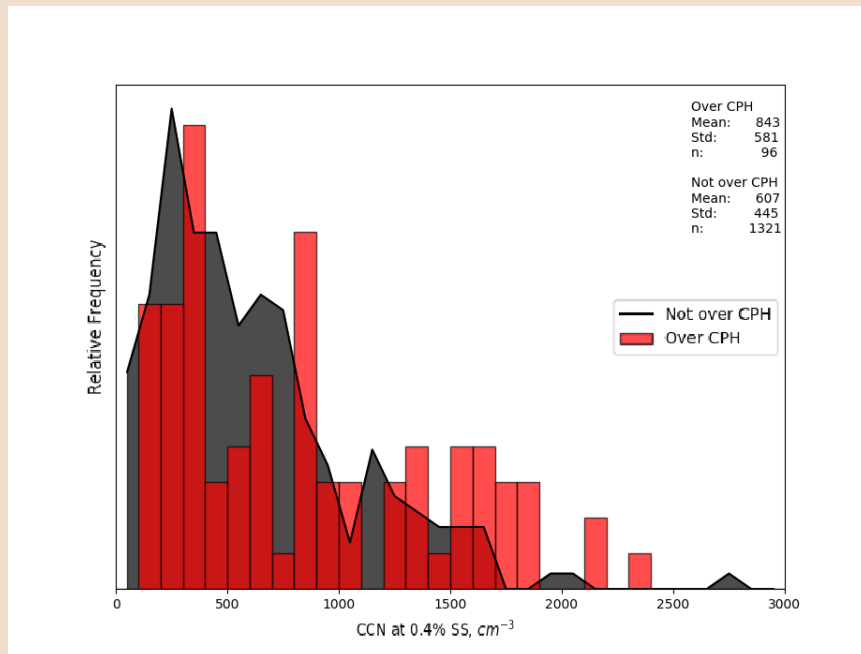


Figure 6: Normalized histogram for air masses passing over CPH (bars) and not passing over CPH (line) for CCN concentration at 0.4 % SS. Hourly data with data labeled according to the analysis of HYSPLIT-trajectory, "over/not over CPH", with every hour between 3 hours before and 3 hours after label same as the trajectory.

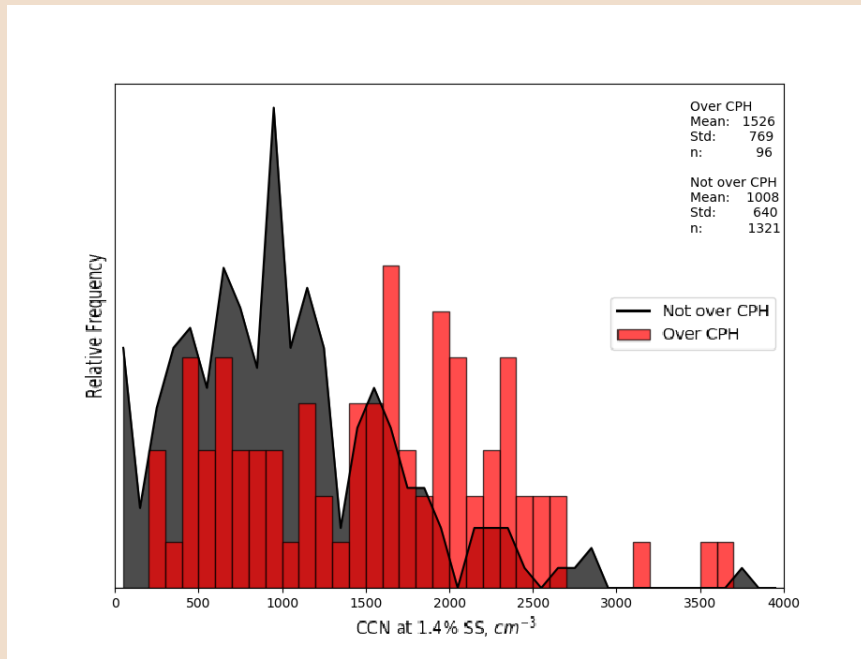


Figure 7: Normalized histogram for air masses passing over CPH (bars) and not passing over CPH (line) for CCN concentration at 1.4 % SS. Hourly data with data labeled according to the analysis of HYSPLIT-trajectory, "over/not over CPH", with every hour between 3 hours before and 3 hours after label same as the trajectory.

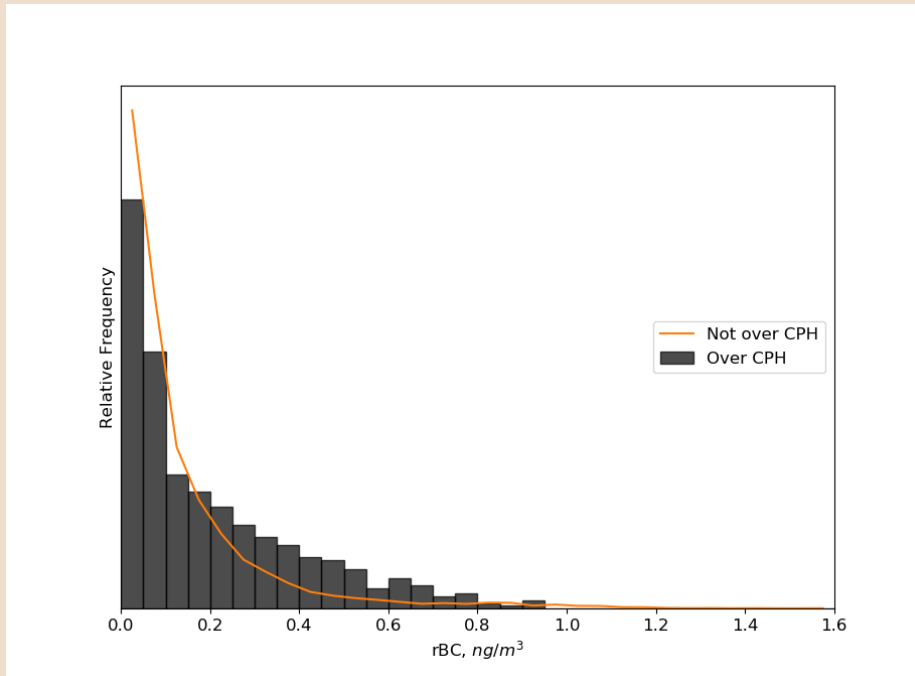


Figure 8: Normalized histograms for air masses passing over CPH (bars) and not passing over CPH (line) for rBC mass concentration, 1 minute data.

Table 2: Means and standard deviation of hourly data of CCN concentration at supersaturations between 0.1-1.4 % measured at the rural station Vavihill. Unit cm^{-3}

Mean CCN at SS:	"With CPH"	"Without CPH"
0.10%	218 ± 155	162 ± 132
0.15%	430 ± 290	327 ± 230
0.20%	583 ± 408	444 ± 313
0.25%	675 ± 490	519 ± 366
0.30%	741 ± 537	569 ± 402
0.35%	796 ± 565	610 ± 431
0.40%	843 ± 581	648 ± 455
0.50%	969 ± 651	717 ± 495
0.70%	1150 ± 679	831 ± 552
1.00%	1352 ± 719	962 ± 611
1.40%	1526 ± 769	1076 ± 657

The CCN data is represented in table 2. The mean CCN for SS between 0.1-1.4 % all show a higher amount of CCN for the air masses that passed Copenhagen with differences between 30-42 %.

This similarity, in the rBC mass concentration, NO_x concentration and CCN concentration, further indicates the air masses being influenced by urban emissions as indicated by the total number of particles. Although, it cannot be concluded that the difference is a direct effect of the influence of Copenhagen, as with the total number of particles.

As can be seen in figure 9, the concentration of CCN for a supersaturation of 0.4 % have a positive correlation with number concentration of particles with diameter larger than 60 nm. The linear regression has a slope of 0.985 for air masses not passing over Copenhagen and 1.126 passing over Copenhagen. This linear regression has R^2 -values of 0.751 for over Copenhagen and 0.703 not over Copenhagen, which corresponds to fairly good approximations. For the concentration of CCN for a supersaturation of 1.4 % (figure 10) there is a positive correlation with slopes of 0.963 for air masses not passing over Copenhagen and 0.992 passing over Copenhagen, with R^2 -values of 0.817 and 0.846 respectively. A relation with slope 1 indicates that for each extra particle, one more particle is activated as CCN and the diameter that this occurs is often referred to as the diameter of activation. This gives an approximate minimum diameter of activation of 60 nm at 0.4 % SS and 40 nm at 1.4 % SS. These correlations partly explain the difference in CCN between air masses passing and not passing over Copenhagen, since the correlations indicates that the amount of CCN increases with number of particles with a larger diameter than the diameter of activation. Hence, the higher concentration of particles the higher CCN concentration.

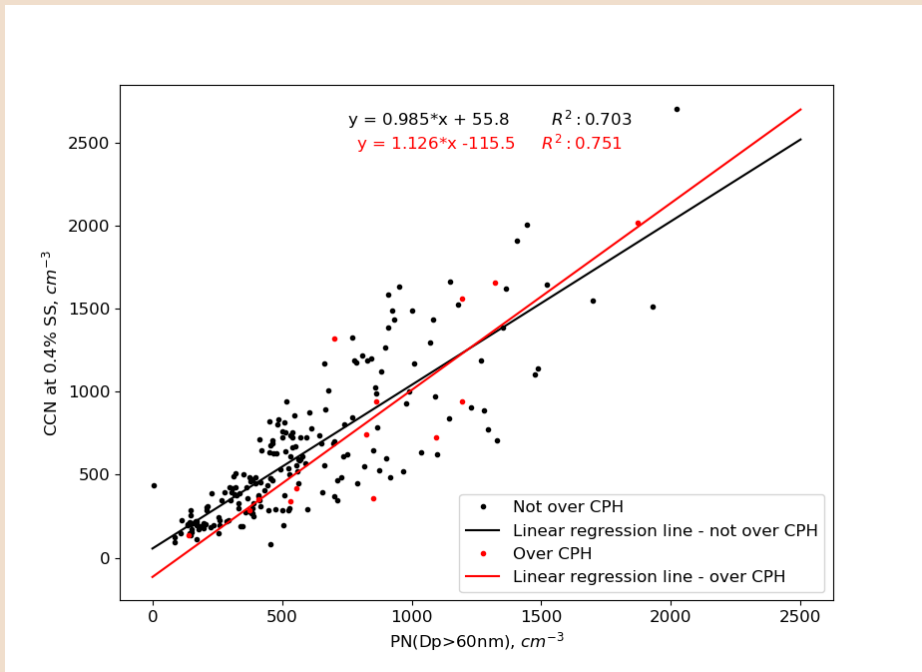


Figure 9: The CCN concentration at 0.4 % SS as a function of number of particle with a diameter larger than 60 nm. The lines represents the linear regression between "over Copenhagen" (red) and "not over Copenhagen" (black).

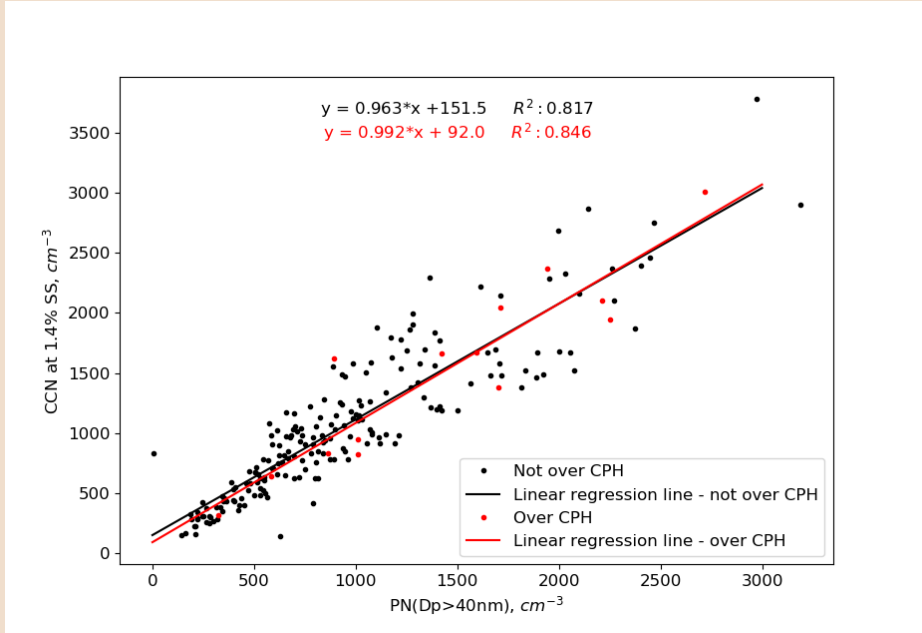


Figure 10: The CCN concentration at 1.4 % SS as a function of number of particle with a diameter larger than 40 nm. The lines represents the linear regression between "over Copenhagen" (red) and "not over Copenhagen" (black).

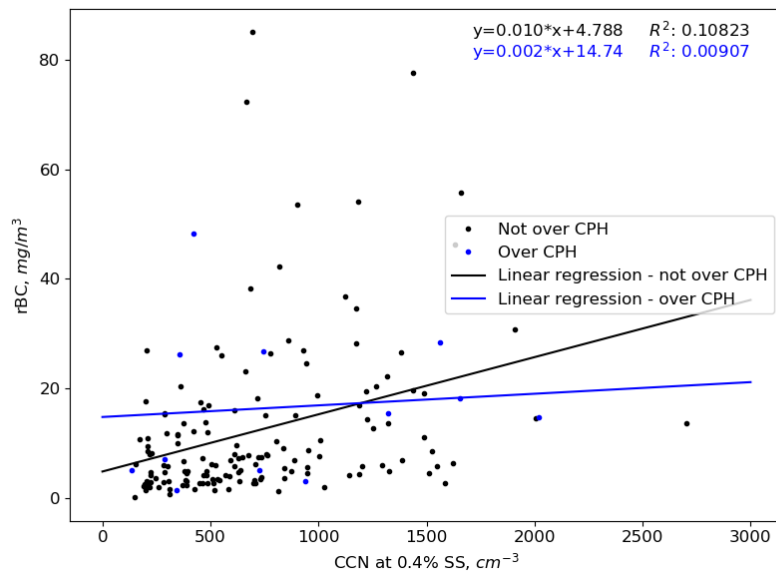


Figure 11: The rBC mass concentration as a function of the CCN concentration at 0.4 % SS. The lines represents the linear regression between "over Copenhagen" (blue) and "not over Copenhagen" (black).

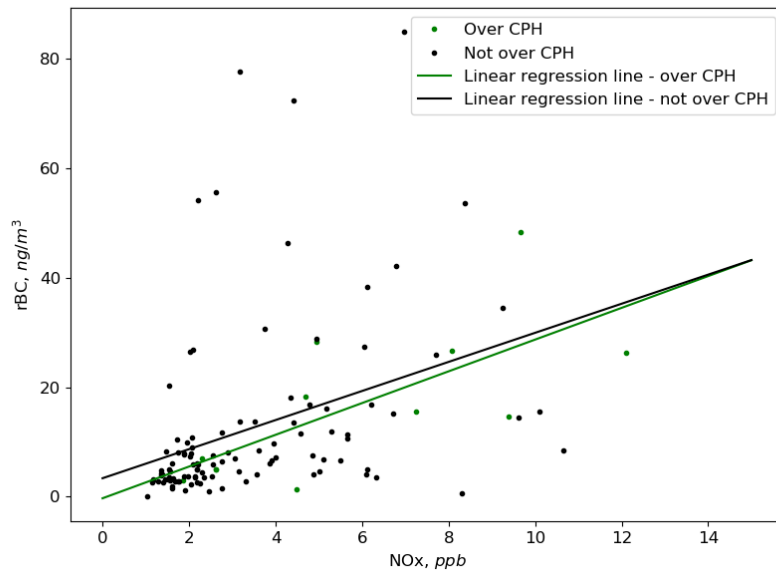


Figure 12: The rBC mass concentration as a function of the NOx concentration. The lines represents the linear regression between "over Copenhagen" (green) and "not over Copenhagen" (black).

The activation diameter at 0.4 % SS is however lower than the expected. The origin of this deviation is hard to determine. Sources of error to account for this deviation is the instruments (CCNC and DMPS) showing a higher number of counts than the actual number of particles. If either of the instrument have measurement errors the relation will be affected and thus might give the resulting deviation. The most probable cause is that the CCNC count to many CCN, which may be due to the supersaturation being higher than the 0.4% that is indicated by the instrument.

The linear regression for the relation between rBC mass concentration and CCN concentration at 0.4 % SS, figure 11, has a slope of 0.002 for the air masses passing over Copenhagen. This shows that the amount of rBC in the aerosol do not directly affect the number concentration of CCN. However, the fit has a $R^2 = 0.009$ which corresponds to a linear fit not being the a good approximation for the relation between rBC mass concentration and CCN concentration at 0.4 % SS. This is further supported by the linear regression for air masses not passing over Copenhagen which has a $R^2 = 0.108$ and a slope of 0.010.

The relation between the rBC mass concentration and NO_x concentration is shown in figure 12. The linear regression has a slope of 0.4836 and 0.4443 for air masses passing and not passing Copenhagen respectively. This correlation shown that the ratio of NO_x to rBC in the aerosol would be similar for all air masses. The fit of the air masses not passing over Copenhagen is however not a good approximation since $R^2 = 0.1309$ whereas the linear fit for the air masses passing over Copenhagen is a much better, but still not optimal, approximation with a $R^2 = 0.5002$. The correlations is highly affected by the low amount of data-points in figures 9-12. This results in the uncertainty of the linear correlation becoming very high. A larger dataset over a longer period of time would provide a more reliable conclusion. The resolution of 6-hour intervals does also present a limitation for the statistical credibility. As all air masses for the three hours before to the three hours after the time for the modeled trajectory are labeled according to the trajectory path, it is most likely some air masses that were classified wrongly. This is due to that the air is constantly varying due to changes in weather conditions, which is not taken into account. These limitations are not only specific to the correlations but are consequently not included in the calculations of the result.

In summation, there is a noticeable difference in the number of particles with a diameter between 3-900 nm, the proportion of rBC (soot) mass concentration and CCN concentration. The difference with and without influences from Copenhagen is not statistically significant due to the large variations in the data. The noticeable difference in CCN concentration and number of particles with a diameter between 3-900 nm have a strong linear correlation which means that an increase in one correlates to an increase in the other. For the other compounds investigated, NO_x and rBC, there was no clear linear correlation found. Due to the low resolution of the air mass trajectories before Copenhagen, insufficient amount of data and no regard of weather conditions, the results of this report are very uncertain and therefore no distinct conclusion can be made. To confirm the conclusions and clarify if there is an influence on the air masses from the urban emission of Copenhagen further investigations with measurements over a longer period of time should be made.

References

- [1] William C. Hinds. *Aerosol technology : properties, behavior, and measurement of airborne particles*. New York: Wiley, 1999. ISBN: 0-471-19410-7.
- [2] J. Haywood and O. Boucher. “Estimates of the direct and indirect radiative forcing due to tropospheric aerosols: A review”. In: *Reviews of Geophysics* 38.4 (2000), pp. 513–543. DOI: 10.1029/1999RG000078. URL: <https://www.scopus.com/inward/record.uri?eid=2-s2.0-0034548018&doi=10.1029%2f1999RG000078&partnerID=40&md5=8470554e158eb1c0684e0ca794ec6410>.
- [3] Roland Akselsson and Mats Bohgard. *Aerosoler*. [Lund]: Lunds Tekniska Högskola : 1994.
- [4] T. Tritscher et al. “Changes of hygroscopicity and morphology during ageing of diesel soot”. In: *Environmental Research Letters* 6.3 (2011), p. 10. ISSN: 1748-9326. DOI: 10.1088/1748-9326/6/3/034026. URL: <http://www.wos.org/doi/10.1088/1748-9326/6/3/034026>.
- [5] Daniel J. Jacob. *Introduction to atmospheric chemistry*. Princeton, N.J.: Princeton University Press, 1999. ISBN: 0-691-00185-5.
- [6] O. Boucher et al. “Clouds and Aerosols”. In: *Climate Change 2013: The Physical Science Basis. Contribution of Working Group I to the Fifth Assessment Report of the Intergovernmental Panel on Climate Change*. Ed. by T.F. Stocker et al. Cambridge, United Kingdom and New York, NY, USA: Cambridge University Press, 2013. Chap. 7, pp. 571–658. ISBN: ISBN 978-1-107-66182-0. DOI: 10.1017/CB09781107415324.016. URL: www.climatechange2013.org.
- [7] Robert J. Charlson et al. “Reshaping the Theory of Cloud Formation”. In: *Science* 292.5524 (2001), pp. 2025–2026. DOI: 10.1126/science.1060096.
- [8] C. L. Reddington et al. “Primary versus secondary contributions to particle number concentrations in the European boundary layer”. In: *Atmospheric Chemistry and Physics* 11.23 (2011), pp. 12007–12036. DOI: 10.5194/acp-11-12007-2011. URL: <https://www.scopus.com/inward/record.uri?eid=2-s2.0-83455231344&doi=10.5194%2facp-11-12007-2011&partnerID=40&md5=f5b24d28926f50adda1e5959c2fd7e8f>.
- [9] Joachim Curtius. “Nucleation of atmospheric aerosol particles”. In: *Comptes Rendus Physique* 7.9 (2006), pp. 1027–1045. ISSN: 1631-0705. DOI: <https://doi.org/10.1016/j.crhy.2006.10.018>. URL: <http://www.sciencedirect.com/science/article/pii/S1631070506002301>.
- [10] C. Wittbom et al. “Cloud droplet activity changes of soot aerosol upon smog chamber ageing”. In: *Atmospheric Chemistry and Physics* 14.18 (2014), pp. 9831–9854. DOI: 10.5194/acp-14-9831-2014. URL: <https://www.scopus.com/inward/record.uri?eid=2-s2.0-84901948343&doi=10.5194%2facp-14-9831-2014&partnerID=40&md5=9cffb82d83f27baf08f50a44efe22ca6>.
- [11] F. Wang et al. “Particle formation events measured at a semirural background site in Denmark”. In: *Environmental Science and Pollution Research* 20.5 (2013), pp. 3050–3059. DOI: 10.1007/s11356-012-1184-6. URL: <https://www.scopus.com/inward/record.uri?eid=2-s2.0-84876729934&doi=10.1007%2fs11356-012-1184-6&partnerID=40&md5=45dc0d697b34776f5e2950d5cb0bad0a>.

- [12] R. Janson and H. C. Hansson. “Luftföroreningar -från utsläpp till effekt”. Stockholm, 2003. URL: <http://www.fysik.su.se/~milstead/teaching/2014/fk4024/Luftf%C3%B6roreningar%20JoH.pdf>.
- [13] Qiang Zhang et al. “Impact of aerosol particles on cloud formation: Aircraft measurements in China”. In: *Atmospheric Environment* 45.3 (2011), pp. 665–672. ISSN: 1352-2310. DOI: <https://doi.org/10.1016/j.atmosenv.2010.10.025>. URL: <http://www.sciencedirect.com/science/article/pii/S1352231010009003>.
- [14] R. R. Rogers and Man Kong Yau. *A short course in cloud physics*. International series in natural philosophy ; 113. Oxford ; Butterworth-Heinemann, 1989. ISBN: 0-7506-3215-1 978-0-7506-3215-7.
- [15] Figure. Apr. 2008. URL: https://en.wikipedia.org/wiki/K%C3%B6hler_theory#/media/File:Kohler_curves.png.
- [16] U. Dusek et al. “Size Matters More Than Chemistry for Cloud-Nucleating Ability of Aerosol Particles”. In: *Science* 312.5778 (2006), pp. 1375–1378. DOI: 10.1126/science.1125261. URL: <http://science.sciencemag.org/content/sci/312/5778/1375.full.pdf>.
- [17] Nicole Riemer et al. “Estimating black carbon aging time-scales with a particle-resolved aerosol model”. In: *Journal of Aerosol Science* 41.1 (2010), pp. 143–158. ISSN: 0021-8502. DOI: <https://doi.org/10.1016/j.jaerosci.2009.08.009>. URL: <http://www.sciencedirect.com/science/article/pii/S0021850209001487>.
- [18] E. Weingartner, H. Burtscher, and U. Baltensperger. “Hygroscopic properties of carbon and diesel soot particles”. In: *Atmospheric Environment* 31.15 (1997), pp. 2311–2327. ISSN: 1352-2310. DOI: [https://doi.org/10.1016/S1352-2310\(97\)00023-X](https://doi.org/10.1016/S1352-2310(97)00023-X). URL: <http://www.sciencedirect.com/science/article/pii/S135223109700023X>.
- [19] N. Riemer, H. Vogel, and B. Vogel. “Soot aging time scales in polluted regions during day and night”. In: *Atmospheric Chemistry and Physics* 4 (2004), pp. 1885–1893. ISSN: 1680-7316. DOI: 10.5194/acp-4-1885-2004. URL: <https://www.wos.org/doi/10.5194/acp-4-1885-2004>. URL: <https://www.wos.org/doi/10.5194/acp-4-1885-2004>.
- [20] A. C. Eriksson et al. “Diesel soot aging in urban plumes within hours under cold dark and humid conditions”. In: *Scientific Reports* 7.1 (2017). DOI: 10.1038/s41598-017-12433-0. URL: <https://www.scopus.com/inward/record.uri?eid=2-s2.0-85030118935&doi=10.1038/s41598-017-12433-0&partnerID=40&md5=2e8d30539750cc02e3d2b1be6390f91b>.
- [21] Claes Bernes. *En ännu varmare värld : växthuseffekten och klimatets förändringar*. Monitor (Solna. Svensk utg.), 1100-231X ; 20. Stockholm: Naturvårdsverket, 2007. ISBN: 978-91-620-1261-8 (inb.)
- [22] E. O. Fors et al. “Hygroscopic properties of the ambient aerosol in southern Sweden—a two year study”. In: *Atmospheric Chemistry and Physics* 11.16 (2011), pp. 8343–8361. DOI: 10.5194/acp-11-8343-2011. URL: <https://www.scopus.com/inward/record.uri?eid=2-s2.0-80051753641&doi=10.5194/acp-11-8343-2011&partnerID=40&md5=3366ef3bc0e37dbdaebca1ba0ae70f09>.

- [23] H. Lyamani, F. J. Olmo, and L. Alados-Arboledas. “Light scattering and absorption properties of aerosol particles in the urban environment of Granada, Spain”. In: *Atmospheric Environment* 42.11 (2008), pp. 2630–2642. ISSN: 1352-2310. DOI: <https://doi.org/10.1016/j.atmosenv.2007.10.070>. URL: <http://www.sciencedirect.com/science/article/pii/S1352231007009703>.
- [24] B. T. Johnson, K. P. Shine, and P. M. Forster. “The semi-direct aerosol effect: Impact of absorbing aerosols on marine stratocumulus”. In: *Quarterly Journal of the Royal Meteorological Society* 130.599 (2006), pp. 1407–1422. ISSN: 0035-9009. DOI: 10.1256/qj.03.61. URL: <https://doi.org/10.1256/qj.03.61>.
- [25] T. B. Onasch et al. “Soot Particle Aerosol Mass Spectrometer: Development, Validation, and Initial Application”. In: *Aerosol Science and Technology* 46.7 (2012), pp. 804–817. ISSN: 0278-6826. DOI: 10.1080/02786826.2012.663948. URL: <https://doi.org/10.1080/02786826.2012.663948>.
- [26] G. C. Roberts and A. Nenes. “A Continuous-Flow Streamwise Thermal-Gradient CCN Chamber for Atmospheric Measurements”. In: *Aerosol Science and Technology* 39.3 (2005), pp. 206–221. ISSN: 0278-6826. DOI: 10.1080/027868290913988. URL: <https://doi.org/10.1080/027868290913988>.
- [27] Bon Ki Ku and Pramod Kulkarni. “Application of fractal theory to estimation of equivalent diameters of airborne carbon nanotube and nanofiber agglomerates”. In: *Aerosol Science and Technology* 52.5 (2018), pp. 597–608. ISSN: 0278-6826. DOI: 10.1080/02786826.2018.1441974. URL: <https://doi.org/10.1080/02786826.2018.1441974>.
- [28] B. Mølgaard et al. “Notably improved inversion of differential mobility particle sizer data obtained under conditions of fluctuating particle number concentrations”. In: *Atmospheric Measurement Techniques* 9.2 (2016), pp. 741–751. DOI: 10.5194/amt-9-741-2016. URL: <https://www.scopus.com/inward/record.uri?eid=2-s2.0-84959542097&doi=10.5194%2famt-9-741-2016&partnerID=40&md5=8b4526ac0daee247bcdaad541f488f30>.
- [29] Web Page. 2018. URL: <http://www.cas.manchester.ac.uk/restools/instruments/aerosol/differential/>.
- [30] E. Z. Nordin et al. “Secondary organic aerosol formation from idling gasoline passenger vehicle emissions investigated in a smog chamber”. In: *Atmospheric Chemistry and Physics* 13.12 (2013), pp. 6101–6116. DOI: 10.5194/acp-13-6101-2013. URL: <https://www.scopus.com/inward/record.uri?eid=2-s2.0-84879924477&doi=10.5194%2facp-13-6101-2013&partnerID=40&md5=1744f775364c336b19e28dfed6d025ff>.
- [31] A. F. Stein et al. “NOAA’s HYSPLIT Atmospheric Transport and Dispersion Modeling System”. In: *Bulletin of the American Meteorological Society* 96.12 (2015), pp. 2059–2077. DOI: 10.1175/bams-d-14-00110.1. URL: <https://journals.ametsoc.org/doi/abs/10.1175/BAMS-D-14-00110.1>.